Asymmetric Structure of the Cystic Fibrosis Transmembrane Conductance Regulator Chloride Channel Pore Suggested by Mutagenesis of the Twelfth Transmembrane Region†

Jyoti Gupta,‡ Alexandra Evagelidis,§ John W. Hanrahan,§ and Paul Linsdell*,‡

Department of Physiology & Biophysics, Dalhousie University, Halifax, Nova Scotia, B3H 4H7, Canada, and Department of Physiology, McGill University, Montréal, Québec, H3G 1Y6, Canada

Received December 12, 2000; Revised Manuscript Received March 6, 2001

ABSTRACT: The cystic fibrosis transmembrane conductance regulator (CFTR) Cl^- channel contains 12 membrane-spanning regions which are presumed to form the transmembrane pore. Although a number of findings have suggested that the sixth transmembrane region plays a key role in forming the pore and determining its functional properties, the role of other transmembrane regions is currently not well established. Here we assess the functional importance of the twelfth transmembrane region, which occupies a homologous position in the carboxy terminal half of the CFTR molecule to that of the sixth transmembrane region in the amino terminal half. Five residues in potentially important regions of the twelfth transmembrane region were mutated individually to alanines, and the function of the mutant channels was examined using patch clamp recording following expression in mammalian cell lines. Three of the five mutations significantly weakened block of unitary Cl^- currents by SCN^-, implying a partial disruption of anion binding within the pore. Two of these mutations also caused a large reduction in the steady-state channel mean open probability, suggesting a role for the twelfth transmembrane region in channel gating. However, in direct contrast to analogous mutations in the sixth transmembrane region, all mutants studied here had negligible effects on the anion selectivity and unitary Cl^- conductance of the channel. The relatively minor effects of these five mutations on channel permeation properties suggests that, despite their symmetrical positions within the CFTR protein, the sixth and twelfth transmembrane regions make highly asymmetric contributions to the functional properties of the pore.

Cystic fibrosis is caused by mutations in a single gene, that encoding the cystic fibrosis transmembrane conductance regulator (CFTR;[1] ref *1*). When CFTR was first identified in 1989, its function was unknown, although homology with other members of the ATP-binding cassette (ABC) family of proteins (*2*, *3*) suggested a role in membrane transport (*1*, *4*). A large body of work has since shown that, while CFTR is a multifunctional protein (*5*), its main role is as a nucleotide-dependent, cyclic AMP-regulated chloride channel (*6*).

The CFTR molecule is formed of two homologous repeats, each consisting of six transmembrane (TM) regions followed by a cytoplasmic nucleotide binding domain (NBD) (Figure 1A). These two halves are joined by a cytoplasmic regulatory (R) domain which contains multiple consensus sequence sites for phosphorylation by protein kinases A and C (Figure 1A; ref *1*). The originally suggested roles of the NBDs and the R domain, in determining channel regulation by ATP binding and hydrolysis and by protein kinase A-dependent phosphorylation (*1*), have subsequently been borne out by a wealth of experimental evidence (*6*, *7*). In contrast, the primary structure of CFTR gave little clue as to the location of the channel pore region through which Cl^- ions permeate, and as such the molecular determinants of the pore remain unclear (*8*, *9*). It is presumed that the pore is formed by multiple TM regions (*8*, *9*). Indeed, there is strong evidence that TM6 plays a key role in forming the pore and determining its functional properties (*10*−*21*). However, despite the persistent view that other TMs must also contribute to the pore (*8*, *9*), strong evidence supporting such a role for any other TM is lacking. The identification of other TM regions which influence channel permeation properties is of key importance in determining the overall architecture of the pore.

CFTR is not structurally related to other classes of Cl^- channels. However, comparison with related ABC proteins which are not ion channels may yield some insight into the organization of the TM regions of CFTR. The transmembrane topology of CFTR is identical to that of the well-characterized ABC protein P-glycoprotein (Pgp), a broad specificity

* To whom correspondence should be addressed. Phone: (902) 494 2265. Fax: (902) 494 1685. E-mail: paul.linsdell@dal.ca.

† This work was supported by grants from the Canadian Institutes of Health Research (CIHR) MT-15397 (to P.L.) and MT-12548 (to J.W.H.), and from the Canadian Cystic Fibrosis Foundation (CCFF) to J.W.H. and P.L. J.W.H. is a CIHR senior scientist. P.L. is a CCFF scholar.

‡ Dalhousie University.

§ McGill University.

[1] Abbreviations: ABC, ATP-binding cassette; BHK, baby hamster kidney; CFTR, cystic fibrosis transmembrane conductance regulator; CHO, Chinese hamster ovary; *i-V*, unitary current−voltage; *I-V*, macroscopic current−voltage; NBD, nucleotide binding domain; Pgp, P-glycoprotein; PKA, protein kinase A catalytic subunit; P_O, channel open probability; P_X/P_{Cl}, permeability of anion X relative to Cl^- permeability; R domain, regulatory domain; TES, *N*-tris-(hydroxymethyl) methyl-2-aminoethanesulfonic acid; TM, transmembrane region; V_{rev}, reversal potential.

10.1021/bi002819v CCC: $20.00
Published on Web 05/10/2001

FIGURE 1: Proposed structure of CFTR TMs 6 and 12. (A) Proposed overall topology of CFTR, comprising 12 TM regions, two cytoplasmic NBDs, and the cytoplasmic R domain. TMs 6 and 12 are indicated; note the equivalent positions of these domains in the amino- and carboxy-terminal "halves" of the molecule. (B) Primary amino acid sequences of TMs 6 and 12, aligned according to ref *9*. Both sequences read from extracellular to intracellular. Asterisks indicate those TM6 residues which were proposed, on the basis of substituted cysteine accessibility mutagenesis, to have side chains in contact with the aqueous lumen of the pore (*14*). Note that, in the case of R347, this now appears not to be the case (*49*), hence the asterisk here is bracketed. Those TM12 residues which were mutated in the present study (T1134, M1137, N1138, S1141, and T1142) are indicated by arrows. (C) Western blots of TM12 mutants stably expressed in BHK cells. A total of 25 μg of cellular protein was used in each lane. No CFTR protein was detected in untransfected BHK cells (BHK, left-hand lane). Lines to the left indicate the positions of 122 and 86 kDa molecular weight markers.

export pump which contributes to the phenomenon of multidrug resistance (*22*, *23*). In Pgp, the TM regions form a ring around a central aqueous pore similar to that which exists in ion channels (*24*). Structural studies have stressed the importance of both TM6 and TM12 in forming the binding site for transported substrates (*22*, *23*, *25*). Furthermore, chemical cross-linking experiments have demonstrated a physical proximity of TMs 6 and 12 (*26*). One recent model suggests that in Pgp, TMs 4, 5, 6, 10, 11, and 12 line a central pore and contribute to substrate binding (*27*, *28*), although other models are also consistent with the available data (e.g., *29*).

On the basis of the homologous positions occupied by TMs 6 and 12 in the amino and carboxy terminal halves of the CFTR molecule (Figure 1A) and the similar and important roles played by TMs 6 and 12 in Pgp (see above), it has been suggested that CFTR-TM12, like TM6, may play a role in forming the pore and determining its functional properties (*9*, *13*, *30*). However, there is very little experimental evidence to support such a view (*8*, *13*, *31*), and the relative functional contributions of TMs 6 and 12 remain unknown. We have investigated the role of TM12 by examining the effect of alanine substitutions for five different TM12 residues on a number of different pore functional properties. We find that mutations in TM12, in contrast to those in TM6, have little effect on channel permeation properties, suggesting that TMs 6 and 12 make highly asymmetric contributions to the pore.

EXPERIMENTAL PROCEDURES

Choice of Mutations. To evaluate the contribution of TM12 to the functional properties of the CFTR pore, we mutated five amino acid residues in this region individually to alanines (Figure 1B). These substitutions were made at each of five of nine consecutive residues in the mid- to extracellular portion of TM12 (Figure 1B). Mutations in the analogous portion of TM6 have previously been shown to affect pore properties such as unitary Cl^- conductance (*11*−*13*, *16*, *21*), anion selectivity (*16*, *20*), and binding of permeant (*21*) and blocking anions (*13*). Furthermore, several residues in this part of TM6 have been shown, on the basis of substituted cysteine accessibility mutagenesis, to be in contact with the aqueous lumen of the pore (*14*; Figure 1B). Residues in TM12 to be mutated were chosen on the basis of two criteria: (i) those with hydroxylated side chains (serine and threonine residues), which have been suggested to interact with permeating anions in Cl^- channels (*9*, *13*, *15*, *32*, *33*; but see ref *16*), and (ii) those which align with TM6 residues which have been suggested to determine CFTR anion selectivity (F337 and T338; ref *16*, *20*, and *21*).

Mutagenesis and Expression of CFTR. Mutagenesis of CFTR in the pNUT vector (*34*) was performed using the QuikChange site-directed mutagenesis kit (Stratagene, La Jolla, CA) as described previously (*20*). The presence of the mutation was confirmed by sequencing the mutated region of the DNA using the T7 Sequenase kit (Amersham, Baie d'Urfe, Québec, Canada).

Subconfluent baby hamster kidney (BHK) and Chinese hamster ovary (CHO) cells were transfected with mutated pNUT-CFTR DNA using the calcium phosphate precipitation method, as described previously (*16*). Individual colonies of transfected cells were selected using methotrexate [Faulding (Canada) Inc., Vaudreuil, Québec, Canada; 500 μM for BHK cells, 50 μM for CHO cells]. Whole cell extracts were subjected to sodium dodecyl sulfate−polyacrylamide gel electrophoresis and Western blotting, using the M3A7 anti-CFTR monoclonal antibody to verify expression of CFTR, as described previously (*16*).

Electrophysiological Recording. Both single channel and macroscopic CFTR current recordings were made using the excised, inside-out configuration of the patch clamp technique, as described previously (*35*, *36*). Briefly, channels were activated following patch excision by exposure of the cytoplasmic face of the patch to 40−130 nM protein kinase A catalytic subunit (PKA; prepared in the laboratory of Dr. M. P. Walsh, University of Calgary, Alberta, Canada; ref *35*) plus 1 mM MgATP. Pipet (extracellular) and bath (intracellular) solutions usually contained (mM) 150 NaCl, 2 $MgCl_2$, and 10 TES (*N*-tris-(hydroxymethyl) methyl-2-aminoethanesulfonic acid). For anion selectivity measurements (Table 1), the bath solution contained (mM) 154 NaX (where X is the anion being tested), 2 $Mg(OH)_2$, and 10 TES. All solutions were adjusted to pH 7.4 using NaOH. All chemicals were obtained from Sigma Chemical Co. (Oakville, Ontario, Canada) except $NaClO_4$ (Aldrich Chemical Co., Milwaukee, WI). Current traces were filtered at 50 Hz (for

Table 1: Relative Anion Permeabilities for Wild-Type and Mutant CFTR[a]

	wild-type	T1134A	M1137A	N1138A	S1141A	T1142A
Cl	1.00 ± 0.01 (10)	1.00 ± 0.06 (5)	1.00 ± 0.03 (6)	1.00 ± 0.02 (4)	1.00 ± 0.02 (5)	1.00 ± 0.04 (7)
Br	1.37 ± 0.07 (8)	1.42 ± 0.03 (4)	1.61 ± 0.02 (5)*	1.32 ± 0.08 (7)	1.54 ± 0.05 (4)	1.44 ± 0.04 (5)
I	0.83 ± 0.03 (6)	0.85 ± 0.04 (4)	0.88 ± 0.02 (3)	0.83 ± 0.03 (4)	0.78 ± 0.01 (3)	0.86 ± 0.03 (3)
F	0.103 ± 0.007 (9)	0.077 ± 0.008 (3)	0.107 ± 0.014 (3)	0.089 ± 0.005 (4)	0.053 ± 0.003 (7)**	0.094 ± 0.007 (3)
SCN	3.55 ± 0.26 (7)	3.70 ± 0.33 (4)	3.58 ± 0.14 (5)	3.53 ± 0.21 (6)	3.37 ± 0.35 (3)	3.64 ± 0.22 (5)
NO_3	1.58 ± 0.04 (10)	1.62 ± 0.05 (4)	1.60 ± 0.04 (3)	1.58 ± 0.05 (6)	1.57 ± 0.03 (3)	1.64 ± 0.07 (3)
ClO_4	0.25 ± 0.01 (8)	0.22 ± 0.00 (3)	0.29 ± 0.02 (3)	0.44 ± 0.05 (5)**	0.22 ± 0.01 (3)	0.30 ± 0.03 (5)
formate	0.24 ± 0.01 (9)	0.26 ± 0.01 (3)	0.27 ± 0.03 (3)	0.27 ± 0.01 (4)	0.26 ± 0.02 (4)	0.25 ± 0.03 (3)
acetate	0.091 ± 0.003 (10)	0.102 ± 0.021 (3)	0.103 ± 0.011 (3)	0.087 ± 0.022 (3)	0.066 ± 0.007 (4)*	0.086 ± 0.009 (3)

[a] Relative permeabilities (P_X/P_{Cl}) for different anions present in the intracellular solution under biionic conditions were calculated from macroscopic current reversal potentials according to eq 1 (see Experimental Procedures), as described in detail previously (*16*, *20*, *36*). Numbers in parentheses indicate the number of patches examined in each case. Asterisks indicate a significant difference from the corresponding value in wild-type [(*) $P < 0.05$, (**) $P < 0.001$, two-tailed *t*-test].

single channel recording) or 100 Hz (for macroscopic current recording) using an 8-pole Bessel filter, and digitized at 250 Hz. Macroscopic currents were analyzed using pCLAMP6 computer software (Axon Instruments, Foster City, CA), while single channel currents were analyzed using custom-written, pCLAMP-compatible DRSCAN software (*35*).

Macroscopic current−voltage (*I-V*) relationships were constructed using depolarizing voltage ramp protocols, with a rate of change of voltage of 37.5−100 mV s^{-1} (see refs *36* and *37*). All *I-V* relationships shown have been corrected for measured liquid junction potentials of up to 6 mV existing between dissimilar pipet and bath solutions (*35*), and have had the background (leak) current recorded before addition of PKA subtracted digitally, leaving uncontaminated CFTR currents (*20*, *35*−*37*). The current reversal potential, V_{rev}, was estimated by fitting a polynomial function to the *I-V* relationship and was used to estimate the permeability of different anions relative to that of Cl^- (P_X/P_{Cl}) according to the equation

$$P_X/P_{Cl} = \exp(\Delta V_{rev} F/RT) \quad (1)$$

where ΔV_{rev} is the difference between V_{rev} measured under biionic conditions with a test anion X^- and that measured with symmetrical Cl^- containing solutions, and *F*, *R*, and *T* have their usual thermodynamic meanings.

Experiments were carried out at room temperature, 21−24 °C. Mean values are presented as mean ± SEM. For graphical presentation of mean values, error bars represent ± SEM, where this is larger than the size of the symbol. Fitting of data and statistical analyses were carried out using SigmaPlot version 5.0 software (SPSS Inc., Chicago, IL).

RESULTS

Mutagenesis and Expression of CFTR. The CFTR molecule contains two sets of six TM residues (Figure 1A). Five alanine-substitution mutations in TM12 were constructed: T1134A, M1137A, N1138A, S1141A, and T1142A (Figure 1B). Expression of each of these mutants in BHK cells led to the production of both core glycosylated (band B) and fully glycosylated (band C) CFTR protein, as judged by Western blotting (Figure 1C), although in each case the amount of protein produced appeared less than for wild-type (Figure 1C). Expression of these same mutants in CHO cells yielded similar results (data not shown), with the exception that S1141A expression could not be detected. Although the reason for this differential expression in different mammalian cell lines is not known, a similar pattern has previously been observed with some TM6 mutants (*21*). One possibility is that quality control mechanisms may be less stringent in BHK cells which express CFTR protein at such high levels.

Macroscopic Current Properties. Expression of mutant CFTR in BHK cells also led to the appearance of PKA- and ATP-dependent Cl^- currents in excised membrane patches (Figure 2A). These Cl^- currents were used as controls for the investigation of the anion selectivity of different CFTR variants (not shown). Anion selectivity was examined under biionic conditions, with Cl^- present in the extracellular solution and different anions present in the intracellular solution, as described in detail previously (*16*, *20*, *36*; see Experimental Procedures). In almost all cases, the relative permeability of a number of different anions (Br^-, I^-, F^-, SCN^-, NO_3^-, ClO_4^-, formate, and acetate) was not significantly altered in TM12 mutants compared to wild-type (Table 1). Where significant differences were noted, they were not sufficient to cause any deviation from the permeability sequence $SCN^- > NO_3^- \geq Br^- > Cl^- > I^- > ClO_4^- \geq$ formate $> F^- \approx$ acetate.

Figure 2 also shows that macroscopic Cl^- currents carried by each CFTR variant studied were inhibited by the addition of 10 mM SCN^- to the intracellular solution, consistent with relatively tight binding of SCN^- within the channel pore (*12*, *17*, *21*). Inhibition was mildly voltage dependent, as previously described at the single channel level (*12*). However, at negative membrane potentials, inhibition appeared relatively insensitive to voltage in all cases (Figure 2B), consistent with our own single channel data for wild-type CFTR under similar ionic conditions (not shown). Block of N1138A (Figure 2B), as well as T1134A, M1137A, and T1142A (data not shown), appeared somewhat weaker than for wild-type, whereas block of S1141A actually appeared stronger than for wild-type (Figure 2B). Although these inhibitory effects of SCN^- are consistent with block of the channel pore, contribution of some other effect of SCN^- (for example, on channel gating) cannot be ruled out from these macroscopic current recordings (see below). As a result of this uncertainty, these macroscopic current inhibition data were not analyzed in any further detail.

Unitary Current Properties. Expression of wild-type, T1134A, M1137A, N1138A, and T1142A-CFTR in CHO cells led to the appearance of unitary PKA- and ATP-dependent Cl^- channel currents in excised membrane patches (Figure 3A). As described above, S1141A could not be expressed in CHO cells; however, unitary S1141A-CFTR

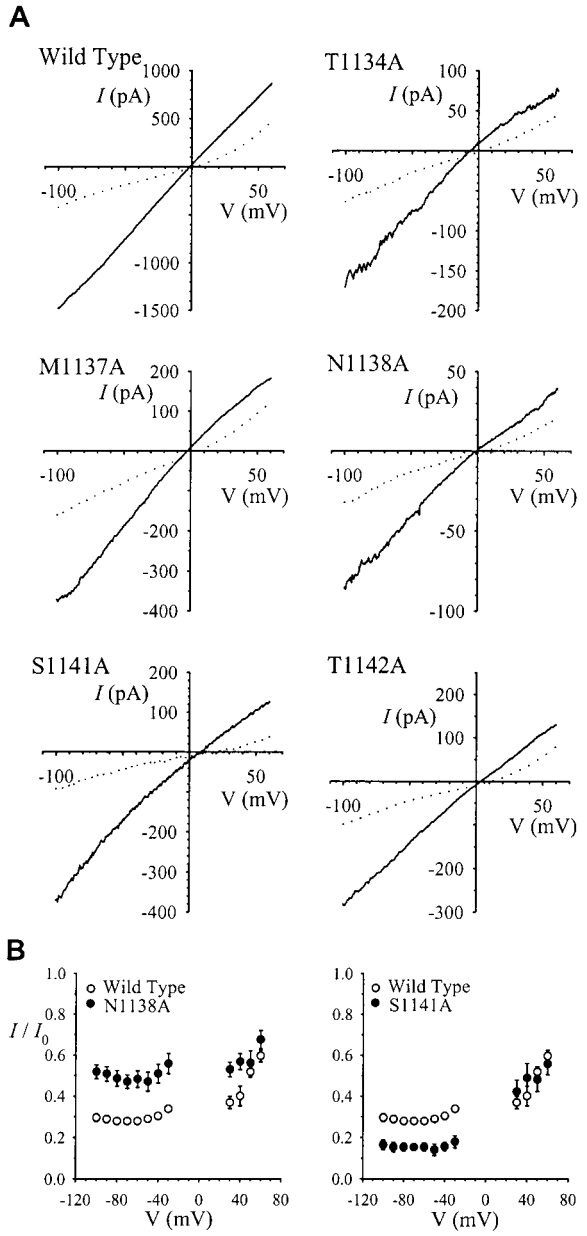

FIGURE 2: Macroscopic Cl^- currents carried by TM12 mutants are inhibited by the addition of SCN^-. (A) Leak-subtracted *I-V* relationships recorded from membrane patches excised from BHK cells expressing each CFTR variant studied, with symmetrical 154 mM Cl^- containing solutions, as described in Experimental Protocols. Currents shown were recorded following attainment of full CFTR channel activation, before (solid lines) and immediately after (dotted lines) addition of 10 mM NaSCN to the intracellular solution. Representative examples of data from 5 to 10 patches in each case. (B) Mean current remaining following addition of 10 mM SCN^- (I/I_0) for wild-type (○), N1138A (●, left panel) and S1141A (●, right panel), shown as a function of voltage. Mean of data from 6 to 10 patches. Block by SCN^- appeared somewhat weakened in N1138A (left), as well as in T1134A, M1137A and T1142A (data not shown, but see Figure 5B), and strengthened in S1141A (right).

currents could be resolved in very small membrane patches excised from BHK cells in the presence of a low concentration of PKA (Figure 3A). The permeation properties of CFTR channels are not expected to be influenced by the cell type in which they are expressed (*36*), although differences in CFTR channel gating between BHK and CHO cell patches have previously been observed (*38*).

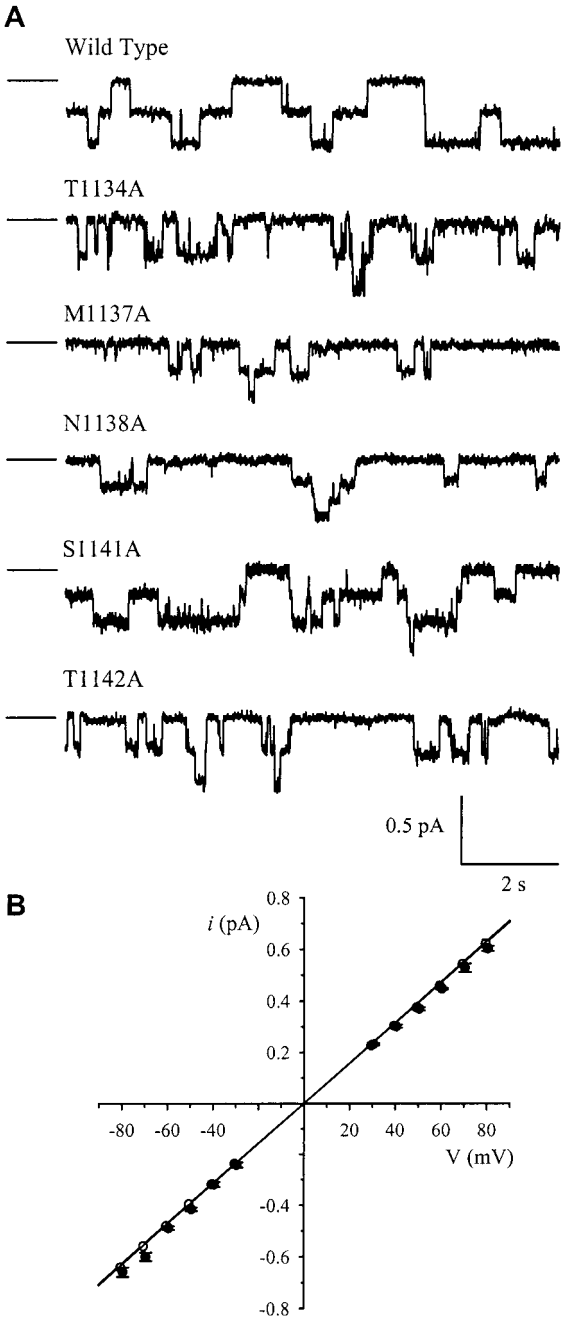

FIGURE 3: Unitary Cl^- currents carried by TM12 mutants. (A) Example single channel currents recorded at a membrane potential of −50 mV with symmetrical 154 mM Cl^- containing solutions. All unitary currents were recorded in CHO cell patches, except S1141A, which was recorded in BHK cell patches. Patches contained two to three active CFTR channels in each case. The line to the left indicates all channels closed. (B) Mean single channel current−voltage relationship for wild-type (○) and N1138A (●). Mean of data from 3 to 18 patches. The form of the current−voltage relationship was similar for all TM12 mutants (not shown).

Unitary *i-V* relationships were recorded for each CFTR channel variant under symmetrical (154 mM Cl^-) ionic conditions. For each of the five TM12 mutants, the form of the *i-V* relationship was very similar to that for wild-type (e.g., N1138A; Figure 3B), and the mean slope conductance was not significantly different to that of wild-type (7.8 ± 0.3 pS; $n = 28$; Figure 4A).

Although the single channel conductance was unaltered in each of these mutants, significant changes in channel

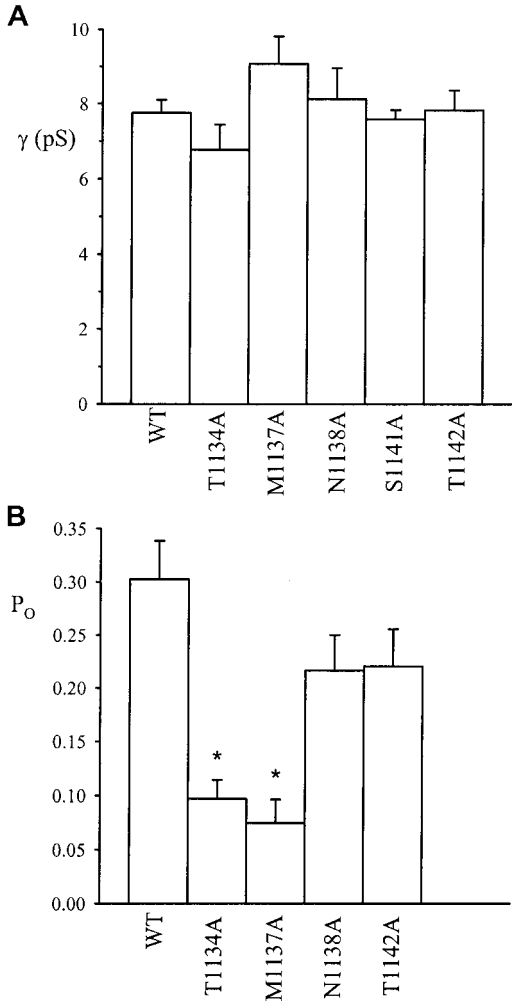

FIGURE 4: Single channel properties of TM12 mutants. (A) Mean single channel conductance (γ), measured from the slope of the single channel current voltage relationship. Mean of data from 28 patches for wild-type, and 6−11 patches for TM12 mutants. (B) Mean channel open probability, measured from recordings made at −50 mV lasting 163−571 s, from CHO cell patches containing one to seven channels. Mean of data from seven to nine patches. Asterisks indicate a significant difference from wild-type (P < 0.001, two-tailed t-test).

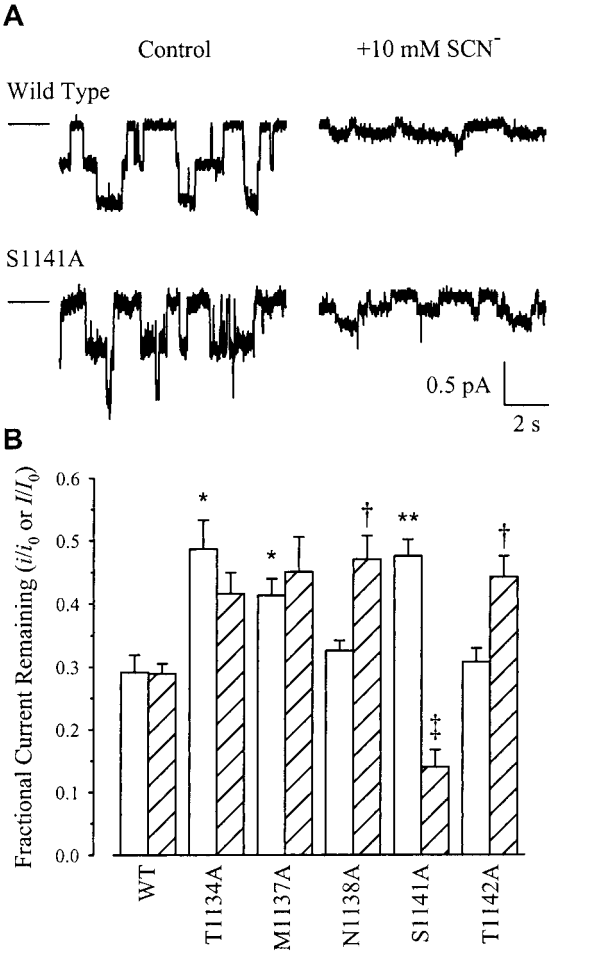

FIGURE 5: Block of unitary Cl^- currents by SCN^-. (A) Unitary currents carried by wild-type and S1141A-CFTR at −50 mV, with symmetrical 154 mM Cl^- containing solutions (control) or after addition of 10 mM NaSCN to the intracellular solution. (B) Mean current amplitude in the presence of 10 mM SCN^- as a fraction of control current amplitude at −50 mV, both at the single channel level (i/i_0; open bars) and at the macroscopic current level (I/I_0; hatched bars; see Figure 2). For wild-type, T1134A, and M1137A, data from these two different methods are in good agreement, however, for other TM12 mutants there is a significant discrepancy [(†) P < 0.01, (‡) P < 0.001, two-tailed t-test]. At the single channel level, significant differences in fractional current remaining compared to wild-type, directly indicative of a weakening of open channel block by SCN^-, are indicated by asterisks [(*) P < 0.01, (**) P < 0.001, two-tailed t-test]. Mean of data from six to nine patches for single channel currents, and 5−10 patches for macroscopic currents.

gating were observed at the single channel level (Figures 3A and 4B). Under steady-state conditions, each of those mutants which could be expressed in CHO cells appeared to have a lower mean channel open probability (P_O) than wild-type, although this difference was only statistically significant for T1134A and M1137A (Figure 4B; P < 0.001, two-tailed t-test). Because of the differences in CFTR channel gating between BHK and CHO cell membrane patches, the P_O of S1141A was not measured.

Binding of permeant anions within the channel pore has previously been described as the most sensitive indicator of changes in pore structure following mutagenesis (*17*). This suggestion was based on the finding that some mutations in TMs 5 and 6 altered block by the permeant anion SCN^- without affecting anion permeability ratios (*17*). Indeed, SCN^- block at the macroscopic current level appeared to be altered in all mutants studied (Figure 2). However, inhibition of macroscopic current by SCN^- could in theory result from a reduction in unitary current amplitude, channel open probability, or the total number of active channels. To examine more directly the effect of mutations in TM12 on anion binding within the pore, block of single channel currents by 10 mM intracellular SCN^- was examined at −50 mV (Figure 5A), a voltage at which block of macroscopic current was relatively strong in all cases (Figure 2). Although no information on the voltage dependence of SCN^- block is obtained in this way, we have previously used this same protocol to show directly that intrapore anion binding is altered in the TM6 mutants F337S and T338A (*21*). Consistent with the results shown in Figure 2, unitary currents carried by all five mutants examined were blocked by SCN^-. However, the degree of block was significantly reduced in T1134A, M1137A, and S1141A compared to wild-type (Figure 5). Thus in these three mutants, SCN^- binding within the pore, as assayed directly by changes in unitary current

amplitude, appears to be weakened. However, there is an obvious discrepancy between these single channel results and the macroscopic current results of Figure 2, as illustrated directly in Figure 5B. For wild-type CFTR, as well as for T1134A and M1137A, the inhibitory effects of 10 mM SCN^- at −50 mV were the same at the macroscopic and single channel levels (Figure 5B). However, for N1138A, S1141A, and T1142A, different degrees of inhibition were observed, suggesting that SCN^- has some other effect on these mutants which is both distinct from the observed reduction in unitary current amplitude and absent in wild-type CFTR. Since the single channel results report the isolated effects of SCN^- on unitary current amplitude, which is presumably determined by the relative tightness of SCN^- binding within the pore, we believe that the reduced apparent SCN^- binding affinity suggested by the single channel results with T1134A, M1137A, and S1141A is the best reporter of altered pore function in these mutants.

DISCUSSION

Architecture of the CFTR Pore. Ion channels allow the passage of ions across membranes by forming an aqueous pathway through which the ions pass. The functional properties of these channel pores are determined by the interactions between permeating ions and those parts of the channel molecule which line the pore. In most cases, the pore is lined by several homologous regions of the channel protein, contributed either by a homologous region in different subunits (as in ligand gated channels; ref *32*) or by repeated motifs within a single polypeptide (as in voltage gated Na^+ and Ca^{2+} channels; ref *39*). In CFTR, it is clear that TM6 plays a key role in forming the pore and determining its permeation properties (*8*, *9*, *20*; see the introductory portion of this paper). However, strong evidence supporting a similar role for any other TM is currently lacking (*8*), and as a result the overall architecture of the pore remains unclear.

On the basis of both the apparent symmetry between the two halves of the CFTR molecule (Figure 1A) and the similar transmembrane topology of CFTR and Pgp (see the introductory portion of this paper), it has been quite logically proposed that TM12, like TM6, might play an important role in forming the CFTR channel pore (*9*, *13*). However, the present results suggest that the contributions of TM6 and TM12 in determining functional pore properties are highly unequal.

Molecular Determinants of Channel Conductance. Mutation of a number of different TM6 residues has previously been shown to alter the unitary Cl^- conductance of CFTR [R334 (*11*); K335 (*12*); F337 (*21*); T338 (*16*); S341 (*13*); R347 (*12*); R352 (*18*)]. The most dramatic changes have been reported for mutations in the central region of TM6 (F337, T338, and S341), perhaps because this part of TM6 contributes to a narrow region of the pore where permeating Cl^- ions interact most strongly with residues lining the walls of the pore. Alanine substitution for these three TM6 residues has been shown to strongly affect conductance, which is greatly reduced in F337A (*21*) and S341A (*13*), and significantly increased in T338A (*16*). In contrast, alanine substitution for the corresponding TM12 residues, M1137, N1138, and S1141 (Figure 1B), as well as for T1134 and T1142, did not significantly alter unitary conductance (Figure 3). Previously, a more dramatic mutation at one of these residues (T1134F) was shown to cause a slight reduction in unitary conductance (*13*).

Molecular Determinants of Anion Selectivity. Mutations in most parts of the putative CFTR pore region do not strongly affect anion selectivity (*8*, *17*). However, mutations at adjacent TM6 residues F337 and T338 do lead to strong changes in the permeability sequence (*16*, *20*), suggesting that anion selectivity is determined primarily at a localized pore region close to these residues. In cation selective channels, selectivity is determined at a "selectivity filter" in the pore, which is formed by a ring of residues contributed by different but analogous regions of the channel protein (*40*, *41*). We therefore considered whether analogous regions of TMs 6 and 12 might contribute to CFTR anion selectivity. However, as summarized in Table 1, TM12 mutations M1137A and N1138A did not alter the anion selectivity sequence, in stark contrast to the corresponding TM6 mutations F337A (*20*) and T338A (*16*). Alanine substitution of the other TM12 residues T1134, S1141, and T1142 had similarly minor effects on selectivity (Table 1).

Molecular Determinants of Anion Binding. Anion binding has previously been described as a key feature of the CFTR channel pore (*8*, *21*), consistent with the notion that permeating anions interact transiently with discrete intrapore binding sites as they permeate through the channel. Intrapore anion binding was assayed by measuring the block of Cl^- currents by SCN^-, which is known to bind relatively tightly within the CFTR channel pore (*12*, *17*). A similar approach has been used to identify amino acid residues in TMs 5 and 6 which influence anion binding (*17*, *21*).

A striking discrepancy between the effects of SCN^- on macroscopic and single channel currents was observed for some mutants (Figure 5B). We suggest that this reflects the fact that SCN^- has some effect on these mutants which is absent in wild-type CFTR. Since the single channel results shown in Figure 5 report changes in intrapore anion binding in isolation, we consider these results the best indicator of altered pore function in CFTR mutants. In contrast, the other effects which we presume contribute to the net inhibition by SCN^- at the macroscopic level could result from a nonpore effect, such as an SCN^--induced change in channel gating. These findings therefore serve as a caveat in interpreting the macroscopic effects of SCN^- as resulting solely from pore block (e.g., ref *17*).

Block of unitary Cl^- currents by SCN^- was significantly weakened in T1134A, M1137A, and S1141A compared to wild-type (Figure 5). This effect, which directly reflects altered SCN^- binding within the open channel, suggests that SCN^- binds less strongly within the pores of these mutant channels. This effect did not appear to be a nonspecific result of mutagenesis within TM12, as SCN^- block was unaltered in both N1138A and T1142A. Similar weakening of SCN^- block was previously observed in the TM6 mutants F337S and T338A (*21*). The ability of mutations at different sites within TM12 to affect SCN^- block suggests that this region does indeed contribute to anion binding within the pore, and hence that TM12 does play a minor role in forming the pore, consistent with a previous report (*13*). However, based on the present results, a more indirect effect of these mutations cannot be ruled out. Since these same mutations have no strong effect on anion selectivity or Cl^- conductance (see

above), these results also support the assertion that anion binding is the most sensitive reporter of subtle changes in CFTR pore architecture (*17*). This may at least in part result from the presence of multiple anion binding sites within the pore.

Role of TM12 in Channel Gating. Although the TM12 mutants studied here had relatively minor effects on the permeation properties of the channel, a strong effect on channel gating was observed. Mean channel P_O under steady-state conditions was reduced to 32% of wild-type levels in T1134A, and to 25% of wild-type in M1137A (Figures 3A and 4B). A similar trend was observed in N1138A and T1142A (Figure 4B), although in these cases the reduction in mean P_O was not statistically significant ($0.05 < P < 0.15$ in both cases, two-tailed *t*-test).

The roles of the TM regions in channel gating has so far received little attention. A point mutation in TM11 (S1118F) was recently shown to cause a dramatic reduction in mean channel open burst duration, implying a decrease in the stability of the channel open state (*42*). However, in this case, the effect on channel P_O was not reported. Mutations in TMs 5 and 6 have previously been shown to reduce the sensitivity of whole cell CFTR currents to activation by agents which increase intracellular cyclic AMP (*17*), although the relationship between such an effect and the steady-state channel gating studied here is not clear.

Gating of the CFTR channel is thought to be controlled by ATP binding and hydrolysis by the two cytoplasmic NBDs (*7*), although how this signal is transduced into a conformational change which opens and closes the channel is not known. Given its proximity to NBD2 in the primary structure of the CFTR molecule (Figure 1A), one possibility is that ATP binding and hydrolysis at this NBD causes a direct conformational change in TM12 which is involved in gating of the pore. Although the present results hint at a link between the TM regions and the gate of the CFTR channel pore, more detailed kinetic analyses under different sets of conditions will be required to investigate fully the role of TM12 in gating.

An Overall Assessment of the Effects of Mutations in TM12. The primary aim of this study was to assess the role of TM12 in determining the permeation properties of the CFTR channel pore. To this end, we examined the effects of mutations at five candidate pore-forming residues on three important aspects of pore function: anion selectivity, Cl^- conductance, and anion binding. All three of these properties are drastically altered by mutagenesis of TM6 (*11*−*13*, *16*−*18*, *20*, *21*), indicating that TM6 plays a central role in forming the pore and controlling anion permeation. In comparison, the effects of TM12 mutations observed here are very minor.

Since only a single mutation at five different residues was studied here, it is possible that different amino acid substitutions and/or mutation of other TM12 residues would have caused a more dramatic change in pore properties. The choice of residues to mutate was based on homology between TMs 6 and 12, as well as residues with hydroxylated side chains (serine/threonine) (see Experimental Procedures). Furthermore, since five out of nine consecutive TM12 residues were mutated, and were selected based on alignment with crucial residues in TM6 (Figure 1B), we consider it unlikely that only the least important TM12 residues were selected. Alanine was chosen as the substituent to minimize disruptions in the structure of the TM, which might be considered more likely to lead to changes at a distance from the site of mutation. Moreover, alanine substitution of key TM6 residues F337, T338, and S341 does lead to significant alteration of a number of pore properties (*13*, *16*, *20*, *21*).

CONCLUSIONS

Comparison of the present results on TM12 with a number of previous studies on TM6 suggests that these apparently homologous regions of the CFTR protein make highly asymmetric contributions to the functional properties of the channel pore. This conclusion is in contrast to prevailing models of the related protein Pgp, where TMs 6 and 12 are thought to make similar (and important) contributions to substrate translocation across the membrane (*22*, *23*, *28*).

The functional asymmetry in the CFTR pore suggested by these results has important implications for pore architecture. One possibility is that the asymmetric contributions of TMs 6 and 12 reflects an asymmetric contribution of the amino- and carboxy-terminal halves of the CFTR molecule. Thus, all of the important determinants of the pore might be found in the amino-terminal half of the molecule. Some evidence exists to support a pore-forming role for TM1 (*10*, *17*, *43*), TM3 (*44*), and TM5 (*17*). Alternatively, TM6 may play a completely dominant role in determining the properties of the pore. This may be more likely if, instead of being a monomer as originally proposed (*45*) and in common with Pgp (*24*, *46*), CFTR channels are formed as dimers (*47*, *48*).

ACKNOWLEDGMENT

We thank Susan Burbridge and Jie Liao for technical assistance.

REFERENCES

1. Riordan, J. R., Rommens, J. M., Kerem, B., Alon, A., Rozmahel, R., Grzelczak, Z., Zielenski, J., Lok, S., Plasvik, N., Chou, J.-L., Drumm, M. L., Iannuzzi, M. C., Collins, F. S., and Tsui, L.-C. (1989) *Science 245*, 1066−1073.
2. Holland, I. B., and Blight, M. A. (1999) *J. Mol. Biol. 293*, 381−399.
3. Klein, I., Sarkadi, B., and Varadi, A. (1999) *Biochim. Biophys. Acta 1461*, 237−262.
4. Hyde, S. C., Emsley, P., Hartshorn, M. J., Mimmack, M. M., Gileadi, U., Pearce, S. R., Gallagher, M. P., Gill, D. R., Hubbard, R. E., and Higgins, C. F. (1990) *Nature 346*, 362−365.
5. Widdicombe, J. H. (2000) *Am. J. Respir. Cell Mol. Biol. 22*, 11−14.
6. Sheppard, D. N., and Welsh, M. J. (1999) *Physiol. Rev. 79*, S23−S45.
7. Gadsby, D. C., and Nairn, A. C. (1999) *Physiol. Rev. 79*, S77−S107.
8. Dawson, D. C., Smith, S. S., and Mansoura, M. K. (1999) *Physiol. Rev. 79*, S47−S75.
9. McCarty, N. A. (2000) *J. Exp. Biol. 203*, 1947−1962.
10. Anderson, M. P., Gregory, R. J., Thompson, S., Souza, D. W., Paul, S., Mulligan, R. C., Smith, A. E., and Welsh, M. J. (1991) *Science 253*, 202−205.
11. Sheppard, D. N., Rich, D. P., Ostedgaard, L. S., Gregory, R. J., Smith, A. E., and Welsh, M. J. (1993) *Nature 362*, 160−164.
12. Tabcharani, J. A., Rommens, J. M., Hou, Y.-X., Chang, X.-B., Tsui, L.-C., Riordan, J. R., and Hanrahan, J. W. (1993) *Nature 366*, 79−82.

13. McDonough, S., Davidson, N., Lester, H. A., and McCarty, N. A. (1994) *Neuron 13*, 623−634.
14. Cheung, M., and Akabas, M. H. (1996) *Biophys. J. 70*, 2688−2695.
15. Linsdell, P., Tabcharani, J. A., Rommens, J. M., Hou, Y.-X., Chang, X.-B., Tsui, L.-C., Riordan, J. R., and Hanrahan, J. W. (1997) *J. Gen. Physiol. 110*, 355−364.
16. Linsdell, P., Zheng, S.-X., and Hanrahan, J. W. (1998) *J. Physiol. 512*, 1−16.
17. Mansoura, M. K., Smith, S. S., Choi, A. D., Richards, N. W., Strong, T. V., Drumm, M. L., Collins, F. S., and Dawson, D. C. (1998) *Biophys. J. 74*, 1320−1332.
18. Guinamard, R., and Akabas, M. H. (1999) *Biochemistry 38*, 5528−5537.
19. Walsh, K. B., Long, K. J., and Shen, X. (1999) *Br. J. Pharmacol. 127*, 369−376.
20. Linsdell, P., Evagelidis, A., and Hanrahan, J. W. (2000) *Biophys. J. 78*, 2973−2982.
21. Linsdell, P. (2001) *J. Physiol. 531*, 51−66.
22. Ambudkar, S. V., Dey, S., Hrycyna, C. A., Ramachandra, M., Pastan, I., and Gottesman, M. M. (1999) *Annu. Rev. Pharmacol. Toxicol. 39*, 361−398.
23. Loo, T. W., and Clarke, D. M. (1999) *Biochem. Cell Biol. 77*, 11−23.
24. Rosenberg, M. F., Callaghan, R., Ford, R. C., and Higgins, C. F. (1997) *J. Biol. Chem. 272*, 10685−10694.
25. Loo, T. W., and Clarke, D. M. (1997) *J. Biol. Chem. 272*, 31945−31948.
26. Loo, T. W., and Clarke, D. M. (1997) *J. Biol. Chem. 272*, 20986−20989.
27. Loo, T. W., and Clarke, D. M. (2000) *J. Biol. Chem. 275*, 5253−5256.
28. Loo, T. W., and Clarke, D. M. (2000) *J. Biol. Chem. 275*, 39272−39278.
29. Jones, P. M., and George, A. M. (2000) *Eur. J. Biochem. 267*, 5298−5305.
30. Zhang, Z.-R., Zeltwanger, S., and McCarty, N. A. (2000) *J. Membr. Biol. 175*, 35−52.
31. Vankeerberghen, A., Wei, L., Teng, H., Jaspers, M., Cassiman, J.-J., Nilius, B., and Cuppens, H. (1998) *FEBS Lett. 437*, 1−4.
32. Lester, H. A. (1992) *Annu. Rev. Biophys. Biomol. Struct. 21*, 267−292.
33. Sansom, M. S. P. (1992) *Eur. Biophys. J. 21*, 281−298.
34. Tabcharani, J. A., Chang, X.-B., Riordan, J. R., and Hanrahan, J. W. (1991) *Nature 352*, 628−631.
35. Hanrahan, J. W., Kone, Z., Mathews, C. J., Luo, J., Jia, Y., and Linsdell, P. (1998) *Methods Enzymol. 293*, 169−194.
36. Linsdell, P., and Hanrahan, J. W. (1998) *J. Gen. Physiol. 111*, 601−614.
37. Linsdell, P., and Hanrahan, J. W. (1996) *J. Physiol. 496*, 687−693.
38. Seibert, F. S., Tabcharani, J. A., Chang, X.-B., Dulhanty, A. M., Mathews, C., Hanrahan, J. W., and Riordan, J. R. (1995) *J. Biol. Chem. 270*, 2158−2162.
39. Guy, H. R., and Durrell, S. R. (1995) In *Ion Channels and Genetic Diseases* (Dawson, D. C., and Frizzell, R. A., Eds.) pp 1−16, Rockefeller University Press, New York.
40. Yang, J., Ellinor, P. T., Sather, W. A., Zhang, J.-F., and Tsien, R. W. (1993) *Nature 366*, 158−161.
41. Doyle, D. A., Cabral, J. M., Pfuetzner, R. A., Kuo, A., Gulbis, J. M., Cohen, S. L., Chait, B. T., and MacKinnon, R. (1998) *Science 280*, 69−77.
42. Zhang, Z.-R., McDonough, S., and McCarty, N. A. (2000) *Biophys. J. 79*, 298−313.
43. Akabas, M. H., Kaufmann, C., Cook, T. A., and Archdeacon, P. (1994) *J. Biol. Chem. 269*, 14865−14868.
44. Akabas, M. H. (1998) *Biochemistry 37*, 12233−12240.
45. Marshall, J., Fang, S., Ostedgaard, L. S., O'Riordan, C. R., Ferrera, D., Amara, J. F., Hoppe, H., Scheule, R. K., Welsh, M. J., Smith, A. E., and Cheng, S. H. (1994) *J. Biol. Chem. 269*, 2987−2995.
46. Loo, T. W., and Clarke, D. M. (1996) *J. Biol. Chem. 271*, 27488−27492.
47. Eskandari, S., Wright, E. M., Kreman, M., Starace, D. M., and Zampighi, G. A. (1998) *Proc. Natl. Acad. Sci. U.S.A. 95*, 11235−11240.
48. Zerhusen, B., Zhao, J., Xie, J., Davis, P. B., and Ma, J. (1999) *J. Biol. Chem. 274*, 7627−7630.
49. Cotten, J. F., and Welsh, M. J. (1999) *J. Biol. Chem. 274*, 5429−5435.

BI002819V